JOURNAL OF THERMOPHYSICS AND HEAT TRANSFER
Vol. 19, No. 2, April–June 2005

Technical Notes

TECHNICAL NOTES are short manuscripts describing new developments or important results of a preliminary nature. These Notes cannot exceed six manuscript pages and three figures; a page of text may be substituted for a figure and vice versa. After informal review by the editors, they may be published within a few months of the date of receipt. Style requirements are the same as for regular contributions (see inside back cover).

Integral Solutions of Droplet Freezing Problems in Hypersonic Melting Ablation

T. F. Zien*
U.S. Naval Surface Warfare Center,
Dahlgren, Virginia 22448

Nomenclature

A_1 = particle temperature profile parameter (third-degree polynomial)
a = particle radius
a_1 = particle temperature profile parameter (second-degree polynomial)
H_a, H_b = functions of $\tilde{h}$, Eqs. (6a) and (6b)
h = average heat convection coefficient
k = thermal conductivity of droplet material
q_{pl} = latent heat of freezing per unit mass of droplet
R = freezing parameter of droplet material, Eq. (11)
r = radial distance from particle center
$\tilde{r}_f$ = dimensionless radial distance of freezing front
T = temperature
T_{pm} = melting (freezing) temperature of particle
t = time
$\tilde{t}_{\mathrm{pc}}$ = dimensionless time when phase change takes place
$\tilde{t}_{\mathrm{pcf}}$ = value of $\tilde{t}_{\mathrm{pc}}$ when freezing front is at $\tilde{r}_f$
V = particle velocity in melt layer
z = vertical distance from the melt–solid interface
$\bar{z}$ = distance from air–melt interface $(z^* - z)$
z^* = melt-layer thickness
α_p = particle thermal diffusivity
γ = specific heats ratio of air
λ_a = resistance parameter of particle motion, $(\rho_2 z^*)/(\rho_p a)$
η_2 = z/z^*, $1 - \bar{z}/z^*$
ρ = density
$\tilde{\upsilon}$ = latent heat parameter

Subscripts

f = end of particle travel in melt layer
m = conditions on ablation surface
p = particle
pc = phase change
1 = condition in air boundary layer, region 1
2 = conditions in melt layer, region 2
∞ = freestream conditions

Superscript

$*$ = conditions at air–melt interface

Presented as Paper 2004-0167 at the AIAA 42nd Aerospace Sciences Meeting, Reno, NV, 5–8 January 2004; received 10 March 2004; revision received 20 September 2004; accepted for publication 21 September 2004.

*Senior Research Scientist, Systems Research and Development Department, Dahlgren Division. Associate Fellow AIAA.

I. Introduction

IN this technical Note, we will describe a simple model for the study of the cooling and subsequent freezing of hot liquid droplets as they travel through the melt layer in the hypersonic melting ablation model proposed by Zien and Wei[1] and Wei and Zien.[2] We will only consider the case of sparse, small particles so that the particle-free ablation model of Refs. 1 and 2 can be used as the basic ablation field (Fig. 1) when the particle effects are considered as a first approximation. Also, for the simplicity of analysis, we will assume that the particles are rigid spheres. The dynamics of the motion of the particle in the melt layer was studied by the author,[3] and the result of the particle trajectory presented in Ref. 3 will be used in the study of the thermal effects of the particle. In a recent investigation,[4] the author used the classical heat balance integral (HBI) method of Goodman[5] to obtain approximate solutions of the heat transfer problem for the cases with and without freezing. This analytical approach to the complex problem has led to an easy identification of the relevant dimensionless parameters of the problem, as well as some simple closed-form solutions. These earlier HBI solutions were based on a simple second-degree polynomial temperature profile for the interior of the particle that satisfies the necessary physical boundary conditions. In the present Note, we will present some new results of particle heat transfer and freezing based on the HBI method with a more appropriate temperature profile inside the spherical particle that satisfies the additional condition of a zero temperature gradient at the center. These new results also make it possible to assess the profile dependence of the HBI solutions for this class of complex aerodynamic heating problems.

II. Model and Analysis

A. Basic Hypersonic Ablation Model

The particle-free hypersonic ablation model as described by Zien and Wei[1] and Wei and Zien[2] will be used as the basis for the study of the particle effects in the first approximation of the case of sparse particles. The structure of the basic model is depicted in Fig. 1, where the coordinate system is fixed on the ablating surface, $z = 0$. The central part of the model is a thin melt layer formed by the molten ablative material, coupled to the air boundary layer on one side and to the ablating solid on the other side. In Refs. 1 and 2, solutions of the fully coupled ablation field have been presented, including the melt layer, in terms of the relevant dimensionless parameters of the model problem. Because we consider only the case of sparse particles of small size (compared to the dimension of the melt layer) in the present Note, the interaction between particles and the effects of particles on the basic ablation field will be neglected.

B. Particle Dynamics

We consider the dynamics of a spherical particle of radius a entering the melt layer of the basic ablation model. The particle has an initial velocity V_i that is on the order of the freestream velocity and is, therefore, very large compared to that of the melt flow in

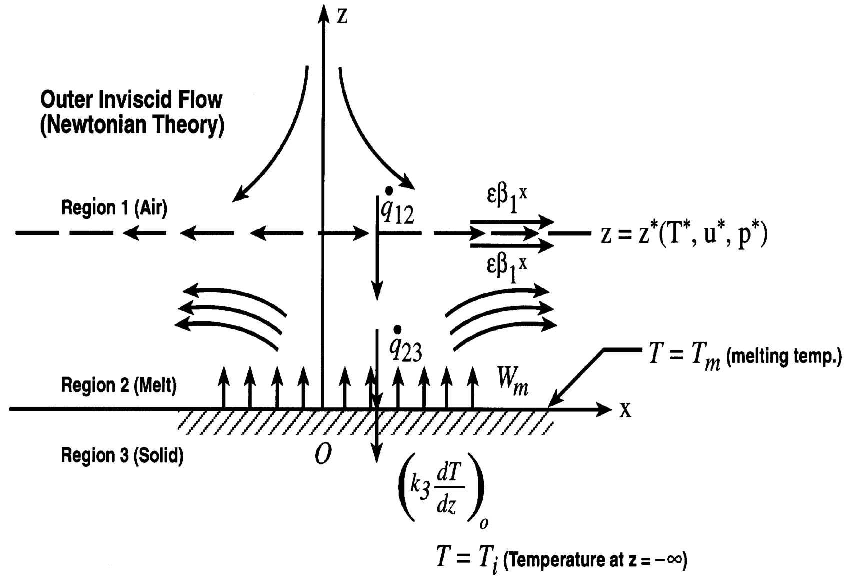

Fig. 1 Basic melting ablation model structure coordinate system fixed on ablation front; see Ref. 1 for complete nomenclature.

the melt layer. As a result, the melt flow can be neglected in the consideration of the particle dynamics.

Results of the particle dynamics calculations, including the particle trajectory, $\bar{z}/z^*(\tilde{t})$, appear in Refs. 3 and 4, and they will be used in the present thermal analysis. We only note here that the motion of the particle in the present model depends only on the deceleration parameter λ_a defined in the Nomenclature.

C. Particle Heat Transfer

For the analysis of heat transfer between the moving particle and the surrounding melt, we make the simplifying assumption of a one-dimensional (radial direction) transient heat conduction inside the particle[3,4] and use an average convective heat transfer coefficient h to represent the heat transfer between the particle and the surrounding melt on the surface of the moving particle. The formulation of the heat transfer problem based on this simplified model is given in Ref. 3 and is also briefly reviewed hereafter for easy reference.

In terms of the spherical coordinates fixed at the center of the particle, the equation of the temperature distribution inside the particle T_p and the appropriate initial and boundary conditions in nondimensional form are as follows:

$$\frac{\partial \tilde{u}}{\partial \tilde{t}} = \tilde{\alpha}_p \frac{\partial^2 \tilde{u}}{\partial \tilde{r}^2} + \tilde{V}\tilde{r}\frac{\mathrm{d}G_2}{\mathrm{d}\eta_2} \tag{1a}$$

$$\tilde{u}(\tilde{r}, 0) = 0 \tag{1b}$$

$$\frac{\partial}{\partial \tilde{r}}\left(\frac{\tilde{u}}{\tilde{r}}\right) \to 0 \qquad \text{as} \quad \tilde{r} \to 0 \tag{1c}$$

$$-\left(\frac{\partial \tilde{u}}{\partial \tilde{r}}\right)_{\tilde{r}=1} = (\tilde{h} - 1)(\tilde{u})_{\tilde{r}=1} \tag{1d}$$

where the nondimensional quantities are defined in the following:

$$\tilde{t} = t/t_f, \qquad \tilde{r} = r/a, \qquad \tilde{\alpha}_p = \alpha_p t_f \big/ a^2$$

$$\tilde{h} = ha/k_p, \qquad \tilde{V} = V\big/\left(z^*/t_f\right) \tag{2a}$$

$$\tilde{u} = \tilde{r}\left\{[T_p - T_2(t)]\big/\left(T^* - T_m\right)\right\}$$

$$G_2(\eta_2) = (T_2 - T_m)\big/\left(T^* - T_m\right) \tag{2b}$$

In the preceding system, $T_2(z)$ is the temperature of the melt layer of the basic particle-free ablation model as obtained in Refs. 1 and 2, and z is related to t through the particle trajectory. The dimensionless heat transfer coefficient $\tilde{h}$ is also known as the Biot number, T_m is the melting temperature of the ablative material, and G_2 is the temperature distribution in the melt layer of the basic particle-free ablation model as given in Refs. 1 and 2.

The additional term on the right-hand side of Eq. (1a) is positive, and it represents an increase of the temperature difference $(T_p - T_2)$ with time as experienced by the traveling particle due to the motion of the particle in the direction of decreasing T_2.

III. HBI Solutions of Droplet Freezing

The HBI method can be conveniently used to provide approximate solutions of Eqs. (1a–1d). The author has presented some HBI solutions of the particle heat transfer problem in Refs. 3 and 4, using a simple second-degree polynomial profile for the temperature in the interior of the particle. In this Note, we will present some additional results based on a more appropriate temperature profile, so that the profile dependence of the HBI solutions for this class of aerodynamic heating problems can also be discussed.

A. Temperature Profiles

In Refs. 3 and 4, the following second-degree polynomial profile was used in the application of the HBI method:

$$\tilde{u} = a_1(\tilde{t})\{1 - [\tilde{h}/(1+\tilde{h})]\tilde{r}\}\tilde{r} \tag{3}$$

Note that this profile corresponds to a nonvanishing temperature gradient at the center of the particle.

To satisfy the exact symmetry condition at the center of the particle, Eq. (1c), the profile should have the symmetry property at the center, that is, a zero temperature gradient. Thus, we will use the following third-degree polynomial profile:

$$\tilde{u} = A_1(\tilde{t})\tilde{r}\{1 - [\tilde{h}/(\tilde{h}+2)]\tilde{r}^2\} \tag{4}$$

which satisfies the symmetry requirement in addition to the surface boundary condition (1d). Here, $A_1(\tilde{t})$ is a profile coefficient to be determined as part of the HBI solution. We note that, with the profile given by Eq. (4), the temperature gradient near the center of the particle will be zero at all times after its entry into the melt layer. Note also that both profiles [Eqs. (3) and (4)] represent temperature fields that are monotonically decreasing of $\tilde{r}$, which is the physically realistic behavior of the temperature inside the droplet.

B. HBI Solutions

Integrating Eq. (1a) across the radius of the particle and substituting the temperature profile Eq. (4) for $\tilde{u}$, we obtain the following ordinary differential equation for the profile coefficient $A_1(\tilde{t})$:

$$\frac{\mathrm{d}A_1}{\mathrm{d}\tilde{t}} + H_a\tilde{\alpha}_p A_1 = H_b \tilde{V} G_2'(\eta_2) \tag{5a}$$

with

$$A_1(0) = 0 \tag{5b}$$

The constants H_a and H_b in Eq. (5a) are functions of the Biot number, and they are defined as

$$H_a = 12[\tilde{h}/(\tilde{h}+4)] \tag{6a}$$

$$H_b = 2[(\tilde{h}+2)/(\tilde{h}+4)] \tag{6b}$$

The solution for the profile parameter $A_1(\tilde{t})$ is readily obtained as follows:

$$A_1(\tilde{t}) = H_b \left\{ \begin{array}{l} e^{-H_a\tilde{\alpha}_p\tilde{t}} - G_2(\eta_2) \\ -H_a\tilde{\alpha}_p e^{-H_a\tilde{\alpha}_p\tilde{t}} \displaystyle\int_{\eta_2}^{1} G_2(\eta_2) e^{H_a\tilde{\alpha}_p\tilde{t}} \frac{\mathrm{d}\tilde{t}}{\mathrm{d}\eta_2}\mathrm{d}\eta_2 \end{array} \right\} \tag{7}$$

We can rewrite Eq. (7) in the following symbolic form:

$$A_1(\tilde{t})/H_b = f(\tilde{t};\, H_a\tilde{\alpha}_p,\, \lambda_a) \tag{8}$$

so that the parametric dependence of the temperature field becomes apparent.

C. Incipient Freezing

The time when freezing first takes place at the surface of the traveling particle is referred to as the incipient freezing time $\tilde{t}_{\mathrm{pc}}$, and it is easily determined by the condition

$$\tilde{u}(1, \tilde{t}_{\mathrm{pc}}) = \frac{T_p(r=a, \tilde{t}_{\mathrm{pc}}) - T_2(\tilde{t}_{\mathrm{pc}})}{T^* - T_m} \tag{9}$$

Equation (9) can be written in the following form with the temperature profile, Eq. (4):

$$A_1(\tilde{t}_{\mathrm{pc}})/H_b = (\tilde{h}+4)\{R - G_2[\eta_2(\tilde{t}_{\mathrm{pc}})]\}/4 \tag{10}$$

where we have introduced the freezing parameter R for droplet freezing in melting ablation, that is,

$$R \equiv (T_{pm} - T_m)\big/\big(T^* - T_m\big) \tag{11}$$

which measures the melting (freezing) temperature difference between the droplet material and the ablative material in terms of the temperature difference across the melt layer.

Solutions of the incipient freezing time can be conveniently obtained graphically by means of Eq. (10) for a given set of values of $(\tilde{h}, H_a\tilde{\alpha}_p, \lambda_a, R)$ and a given basic ablation field (hence, G_2) as follows. The left-hand side of Eq. (10) is first plotted as a function of time by the use of the results of Eq. (7), or Eq. (8), and the right-hand side of Eq. (10) is also plotted as a function of time. The intersection of the two curves then gives an approximate solution of $\tilde{t}_{\mathrm{pc}}$. Of course, the graphical solution so obtained represents only a crude approximation of the incipient freezing time, which can be used as a starting point for a more exact solution of Eq. (10), for example, by an iteration method.

Values of R, of course, vary with droplet materials, and they are in the range (0, 1). Consider the freezing of aluminum oxide droplets in a solid rocket motor exhaust that is impinging on a melting (glassy) ablator under some typical cases of operation in a hypersonic environment ($T_{\mathrm{pm}} \approx 2300^\circ\mathrm{C} \sim 2400^\circ\mathrm{C}$, $T_m \approx 1600^\circ\mathrm{C}$, and $T^* = 2600^\circ\mathrm{C}$), and so we have $R \approx 0.7 \sim 0.8$. Thus, we will focus our consideration and discussion on $R = 0.7$ and 0.8 in this Note.

D. Subsequent Freezing

Subsequent to incipient freezing, the interior of the droplet will begin to freeze as the droplet continues to travel into the colder surrounding melt in the melt layer. In general, the heat balance condition to be imposed on the freezing front must include the effect of latent heat of freezing. Formulation of the general problem of subsequent freezing is given in Ref. 4. We only note that a latent heat parameter $\tilde{\upsilon}$ defined as

$$\tilde{\upsilon} \equiv \frac{\rho_p q_{pl} a^2}{k_p\big(T^* - T_m\big)t_f} \tag{12}$$

determines the importance of the latent heat in the freezing front location. Here, $\tilde{\upsilon}$ is roughly the ratio of the total latent heat contained in the droplet to the total heat released to the melt layer by the droplet through conduction during the time of its travel across the melt layer. An estimate of the value of $\tilde{\upsilon}$ follows.

We consider the freezing of aluminum oxide droplets in a melting ablation field. Here we have[6,7]

$$\rho_p = 4\ \mathrm{g/cm^3}, \qquad a = 2.5\times 10^{-4}\ \mathrm{cm} \tag{13}$$

We estimate the thermal conductivity of Al_2O_3 droplets to be a little less than that of pure aluminum, and so we take $k_p \approx 0.4$ cal/s · cm · °C. We also estimate the specific latent heat of the droplet to be $q_{pl} \approx 278$ cal/g ($\approx$500 Btu/lbm). Finally, for a typical melt layer in the hypersonic melting ablation model, we estimate $T^* - T_m \approx 1000^\circ\mathrm{C}$ and $t_f = 5\times 10^{-6}$ s. Under these conditions, we have

$$\tilde{\upsilon} \approx 3.5\times 10^{-2} \ll 1 \tag{14}$$

Note that larger values of t_f would give even smaller values of $\tilde{\upsilon}$. Therefore, it appears reasonable to assume that the latent heat parameter is typically a small quantity in practical applications. In the present Note, we will present solutions only for the limiting case of small values of latent heat, that is, $\tilde{\upsilon} \to 0$, which is obviously a much simpler problem. It is anticipated that these simple solutions will be useful as a guide to the solutions of the more general droplet freezing problems to be studied later.

E. Freezing Front Location: Limiting Case of Small $\tilde{\upsilon}$

In the limit of $\tilde{\upsilon} \to 0$, both the temperature and its gradient become continuous across the freezing line, and the temperature field is, thus, expected to be smooth within the entire droplet. The freezing front simply becomes a line of constant temperature $T_p = T_{pm}$ that separates the liquid region from the solid region, and a single temperature profile can be used to study the temperature field inside the droplet, including the location of the moving freezing front. We will use the third-degree polynomial, Eq. (4), as the temperature profile for the calculations, and the results will be compared with those of the second-degree polynomial profile.[4]

We are primarily interested in determining the location of the freezing front, $\tilde{r} = \tilde{r}_f(\tilde{t}_{\mathrm{pcf}})$. To proceed, we write the temperature profile as

$$\tilde{u}/\tilde{r} = (T_p - T_2)\big/\big(T^* - T_m\big) = A_1(\tilde{t})\{1 - [\tilde{h}/(\tilde{h}+2)]\tilde{r}^2\} \tag{15}$$

Because $\tilde{r} = \tilde{r}_f$ at $\tilde{t} = \tilde{t}_{\mathrm{pcf}}$, we can rewrite the Eq. (15) as

$$\frac{A_1(\tilde{t}_{\mathrm{pcf}})}{H_b} = \frac{[R - G_2(\eta_{2\mathrm{pcf}})]}{\big\{1 - [\tilde{h}/(\tilde{h}+2)]\tilde{r}_f^2\big\}}\frac{\tilde{h}+4}{2(\tilde{h}+2)} \tag{16}$$

where $\eta_{2\mathrm{pcf}}$ is related to $\tilde{t}_{\mathrm{pcf}}$ through the particle trajectory for a given value of λ_a.

It is, thus, clear from Eq. (16) that, for a given basic ablation field where the melt layer temperature distribution G_2 is given, the freezing front trajectory $\tilde{r}_f(\tilde{t})$ can be expressed parametrically as

$$\tilde{r}_f = \tilde{r}_f(\tilde{t};\, \lambda_a,\, H_a\tilde{\alpha}_p,\, \tilde{h},\, R) \tag{17}$$

As in the case of incipient freezing discussed in Sec. III.C, solutions of $\tilde{t}_{\text{pcf}}$ can also be obtained graphically based on Eq. (16). In fact, when $\tilde{r}_f = 1$, Eq. (16) reduces to Eq. (10), which was used to determine the incipient freezing time $\tilde{t}_{\text{pc}}$. Freezing of the traveling droplet is complete in the melt layer when $\tilde{r}_f = 0$ with $\tilde{t}_{\text{pcf}} \leq 1$. From Eq. (17), we see that the condition of $(\tilde{r}_f, \tilde{t}_{\text{pcf}}) = (0, 1)$, which corresponds to complete freezing at the end of the droplet travel in the melt layer, determines a specific value of $R = R_{\min}$ for a given set of values of the parameters $(\lambda_a, H_a\tilde{\alpha}_p, \tilde{h})$ in a given basic ablation field. Hence, $R_{\min}$ is the minimum value of the freezing parameter, that is, minimum freezing or melting temperature of the droplet material, below which the droplet will not complete the freezing process before it reaches the bottom of the melt layer. The solution of $R_{\min}$ can be easily obtained from Eq. (16) by setting $(\tilde{t}_{\text{pcf}}, \tilde{r}_f, \eta_{2\text{pcf}}) = (1, 0, 0)$, and we arrive at the following remarkably simple result:

$$R_{\min} = A_1(1) \tag{18}$$

This simple, approximate result should be useful in the consideration of material selection for the melting ablation system that involves droplets in the gas stream.

We note here that the special case of $R = 1$ corresponds to the case of droplet melting temperature equal to the temperature of the melt–air interface, which is assumed to be the uniform temperature of the droplet on entry into the melt layer. The droplet freezing is, thus, complete at $\tilde{t} = 0$, and the temperature profile becomes irrelevant in the determination of the interior freezing in this special case.

IV. Results and Discussion

Calculations based on the analysis of Sec. III have been carried out, and the results will be presented and discussed hereafter. The calculations are based on the basic ablation field characterized by the following parameters:

$$\left(\varepsilon, R^*, m, N_m, Pr_1, Pr_2, \bar{\nu}_2 \big/ \nu_1^*\right) = (0.2, 0.4, 0.1, 0.75 \times 10^{-6}, 0.7, 5.0, 0.25 \times 10^{-3}) \tag{19}$$

and the solutions of the basic ablation field are given in Ref. 1. Also, we have used the same values of the parameters, λ_a and $\tilde{h}$, that is, $(\lambda_a, \tilde{h}) = (1, 1)$, in all of the calculations.

We note that because of the simplicity of the results obtained by the HBI method, most calculations require nothing more than the numerical evaluation of some definite integrals.

Also, in the interest of comparing the present results with those of the second-degree polynomial profile of Ref. 4, we will choose the same physical situation, that is, the same values of the parameters $(\tilde{\alpha}_p, \tilde{h})$, for the calculations. In view of the similarity parameters in the approximate HBI solutions of the heat transfer and freezing problems as exhibited in Eqs. (8) and (17), we will use the following values of the parameter $H_a\tilde{\alpha}_p$ in the present calculations, that is, $H_a\tilde{\alpha}_p = (1.2, 0.4)$, which correspond, respectively, to the cases of $H_1\tilde{\alpha}_p = (1.5, 0.5)$, studied in Ref. 4, so that both calculations correspond to the same values of $(\tilde{h}, \tilde{\alpha}_p) = (1, 1/2)$ and $(\tilde{h}, \tilde{\alpha}_p) = (1, 1/6)$, respectively.

A. Incipient Freezing Times

Calculations of the incipient freezing times are easily carried out by the graphic method, as described in Sec. III.C. Results of these calculations are presented in Fig. 2 for three values of the freezing parameter, $R = (0.8, 0.7, 0.52)$. For a fixed value of the thermal diffusivity of the droplet $\tilde{\alpha}_p$, incipient freezing happens earlier for higher values of R, that is, higher droplet freezing temperatures, as physically expected. For a fixed value of R, on the other hand, incipient freezing takes place earlier for larger values of the thermal diffusivity of the droplet, which is also intuitively correct. Note that the case $R = 0.52$ is included here for its significance in representing the case of $R_{\min}$ for complete freezing of the droplet. $R_{\min}$ is, of course, determined by Eq. (18), and the practical procedure used for its evaluation is the same as that used in Ref. 4. Note also that for the second-degree polynomial profile, the value of $R_{\min}$ is 0.54 (Ref. 4).

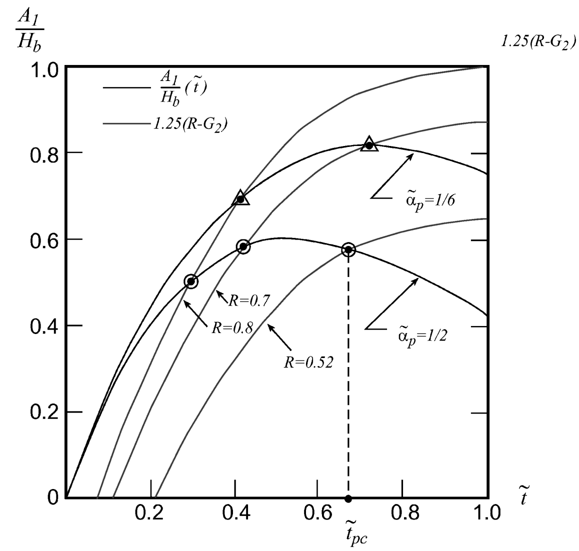

Fig. 2 Determination of incipient freezing times $(\lambda_a, \tilde{h}) = (1, 1)$, third-degree polynomial profile, basic ablation field[1]: $(m, \varepsilon, R^*, N_m, Pr_1, Pr_2, \nu_2/\nu_1) = (0.1, 0.2, 0.4, 0.75 \times 10^{-6}, 0.7, 5.0, 0.25 \times 10^{-3})$.

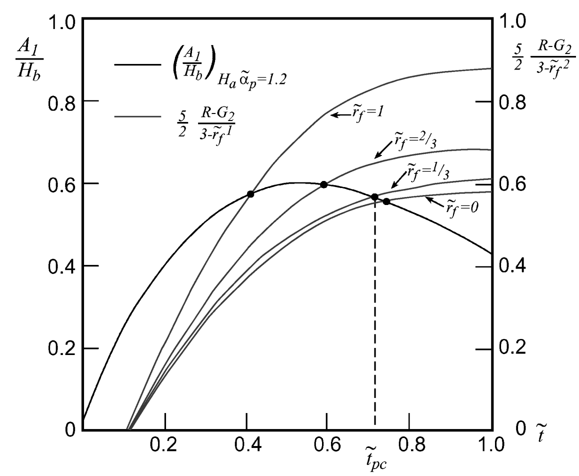

Fig. 3 Interior freezing times $(\tilde{v} \to 0)$, $(\lambda_a, \tilde{h}, \tilde{\alpha}_p, R) = (1, 1, 1/2, 0.7)$, third-degree polynomial profile; same basic ablation field as Fig. 2.

B. Interior Freezing

The location of the freezing front in the interior of the traveling droplet as a function of time can be easily determined by the use of Eq. (16), in the limit of $\tilde{v} \to 0$. Results of the determination of the freezing times $\tilde{t}_{\text{pcf}}$ are shown in Figs. 3 and 4 for $R = 0.7$ and 0.8, respectively, and for four different radial locations, $\tilde{r}_f = 1$, 2/3, 1/3, and 0. Obviously, the curve $\tilde{r}_f = 1$ corresponds to the case of incipient freezing. Note that the freezing times for radii near the center of the droplet, $\tilde{r}_f = 0$, are much closer to each other than those predicted with the second-degree polynomial profile.[4] This is due to the difference in the temperature behavior as specified by the profiles. For the third-degree polynomial profile, the rate of the temperature drop decreases with decreasing radius so that most of the freezing takes place in the early times of the droplet travel. Note that the second-degree polynomial profile does not have the explicit radial dependence of the temperature gradient.

C. Effects of Temperature Profiles

Figure 5 summarizes the results of Figs. 3 and 4 in the form of freezing times as a function of the radial location inside the droplet. It also includes the corresponding results of the previous calculations[4]

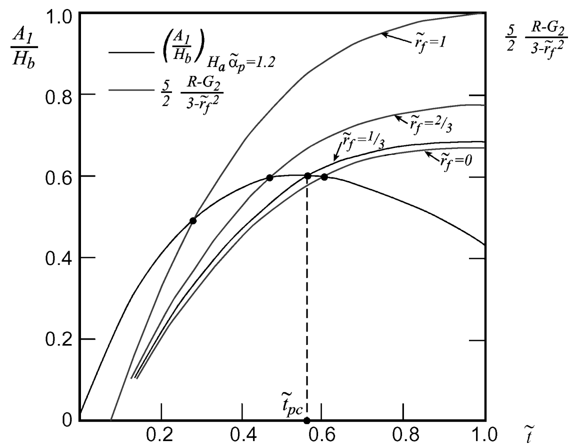

Fig. 4 Interior freezing times ($\tilde{v} \to 0$), $(\lambda_a, \tilde{h}, \tilde{\alpha}_p, R) = (1, 1, 1/2, 0.8)$, third-degree polynomial profile; same basic ablation field as Fig. 3.

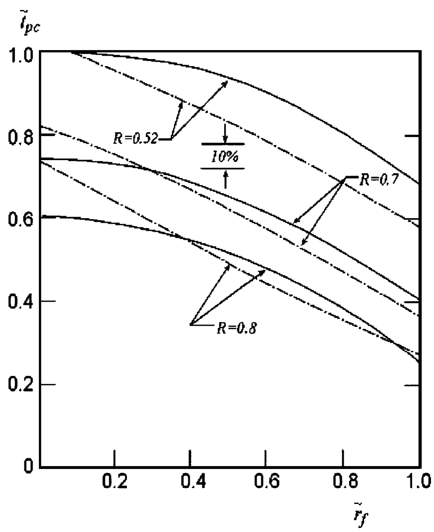

Fig. 5 Interior freezing times ($\tilde{v} \to 0$), profile effects $(\lambda_a, \tilde{h}, \tilde{\alpha}_p) = (1, 1, 1/2)$: ——, third-degree polynomial and –·–, second-degree polynomial; same basic ablation field as Fig. 3.

based on the second-degree polynomial profile with the same values of the parameters, $(\tilde{h}, \tilde{\alpha}_p) = (1, 0.5)$. The profile dependence of the HBI solutions (see, for example, Ref. 8) can, thus, be easily inferred from Fig. 5. Recall that the solid curve with $R = 0.52$ gives the freezing times for the case of minimum R for the present third-degree polynomial profile, and, as such, the droplet center ($\tilde{r}_f = 1$) freezes at $\tilde{t}_{\text{pcf}} = 1$. The result based on the second-degree polynomial profile (broken line) for the same value of $R = 0.52 (< R_{\min} = 0.54)$ shows incomplete freezing, that is, $\tilde{r}_f \approx 0.08$ at $\tilde{t}_{\text{pcf}} = 1$, as expected. For $R = 1$, we expect the result of $\tilde{r}_f = 1$ at $\tilde{t}_{\text{pcf}} = 0$ for both profiles.

The agreement of the results based on the two different profiles is seen to be better than about 10%, in general, except near the center, where the deviation tends to increase with increasing values of the freezing parameter R. This can probably be explained by the pronounced difference in the temperature gradients near the center of the droplet associated with the two profiles. (See Sec. III.A.).

V. Conclusions

The application of the HBI method to the melting ablation problems in the presence of particles and droplets in the hypersonic gas stream is reported in the present Note. Particular emphasis is given to the effects of freezing of the droplets during their passage through the attendant melt layer. An explicit purpose in the study is to assess the effects of profile dependence of the approximate solutions, which is a well-known deficiency of the HBI method.

To this end, a new temperature profile in the form of a third-degree polynomial is used in the present Note, which satisfies the symmetry condition, that is, zero temperature gradient, at the droplet center, as opposed to the second-degree polynomial profile used in the previous study.[4] Results are again obtained in simple analytical form, and the various parameters relevant to the physical phenomena under investigation are easily identified. Thus, the computational labor required to obtain explicit solutions is minimal.

The present results are compared with the corresponding results presented in Ref. 4. The comparison shows a reasonable agreement in the prediction of incipient freezing time and the subsequent freezing times of the droplet interior in general, except near the droplet center where a stronger profile dependence is indicated.

As is well known, the choice of a profile in the application of the HBI method is not unique, and it is, thus, encouraging that the results of its particular application presented in this Note seem to be only weakly dependent on profiles. Note, however, that a good judgment based on physical intuition is still required in the choice of temperature profiles. For example, a temperature profile that is a monotonically decreasing function of the radius in the present problem proves to be essential, as was discussed in Sec. III.A.

On the basis of the results presented here and those of Refs. 3, and 4, it seems that the classical HBI method is capable of providing approximate solutions of this class of melting ablation problems for engineering applications. Obviously, in the absence of exact solutions of the governing equations and relevant experimental data for comparison, the absolute accuracy of these HBI solutions cannot be established. However, the integral method is based on the basic conservation laws of physics, as is well known, and the corresponding results are, thus, believed to have a rational and reliable basis. Moreover, the simplicity and the analytical nature of the solutions are, of course, the primary merits of the method.

Note that the model used in the present Note for the study of droplet freezing problem is a greatly simplified one. However, because such a simplified model problem is amenable to analytical treatment by the simple HBI method and, thus, allows the relevant parameters of the complex physical phenomena to be easily identified, the parametric dependence of the solution can be studied analytically to provide insight to the physical problem with minimal computational effort. Thus, the simple model appears to have merit for use as a first step in the development of practical design tools for thermal protection systems in such hypersonic heating environments.

Acknowledgments

This research was supported by the In-House Laboratory Independent Research Program of the U.S. Naval Surface Warfare Center, Dahlgren Division. This paper is a revised and abbreviated version of AIAA Paper 2004-0167. The author thanks G. Soo Hoo of the U.S. Naval Surface Warfare Center, Dahlgren Division, for the latent heat data for Al_2O_3 droplets used in this Note.

References

[1] Zien, T. F., and Wei, C. Y., "Heat Transfer in the Melt Layer of a Simple Ablation Model," *Journal of Thermophysics and Heat Transfer*, Vol. 13, No. 4, 1999, pp. 450–459.

[2] Wei, C. Y., and Zien, T. F., "Integral Calculations of Melt-Layer Heat Transfer in Aerodynamic Ablation," *Journal of Thermophysics and Heat Transfer*, Vol. 15, No. 1, 2001, pp. 116–124.

[3] Zien, T. F., "Thermal Effects of Particles on Hypersonic Ablation," *Journal of Thermophysics and Heat Transfer*, Vol. 16, No. 2, 2002, pp. 285–288; also AIAA Paper 2001-2883, June 2001.

[4] Zien, T. F., "Effects of Particles and Droplets on Hypersonic Ablation in Thermal Protection Systems," AIAA Paper 2002-5159, Sept./Oct. 2002.

[5] Goodman, T. R., "Application of Integral Methods to Transient Nonlinear Heat Transfer," *Advances in Heat Transfer*, Vol. 1, 1964, pp. 51–122.

[6] Ungar, E. W., "Particle Impacts on the Melt Layer of an Ablating Body," *ARS Journal*, Vol. 30, No. 9, 1960, pp. 799–805.

[7] Lewis, D., and Anderson, L., "Effects of Melt-Layer Formation on Ablative Materials Exposed to Highly Aluminized Rocket Motor Plumes," AIAA Paper 98-0872, Jan. 1998.

[8] Zien, T. F., "Integral Solutions of Ablation Problems with Time-Dependent Heat Flux," *AIAA Journal*, Vol. 16, No. 12, 1978, pp. 1287–1295.